# Molecular dynamics study of diffusion in a bilayer electron gas

S. Ranganathan
*Department of Physics, Royal Military College of Canada, Kingston, Ontario, Canada K7K 7B4*

R. E. Johnson
*Department of Mathematics and Computer Science, Royal Military College of Canada, Kingston, Ontario, Canada K7K 7B4*

K. N. Pathak
*Department of Physics, Panjab University, Chandigarh, India 160014*

(Received 10 December 2001; published 14 May 2002)

Molecular dynamics simulations of strongly coupled, classical electronic bilayers, interacting through the Coulomb potential, have been produced and studied. Values of the plasma coupling parameter $\Gamma$ between 10 and 80 and interlayer separations $d$ from 0.1 to 3.0, (in units of Wigner-Seitz radius), were considered. The simulation results were used to calculate the intralayer and interlayer pair correlation functions and self-diffusion of charged particles in this system. The variation of self-diffusion with $\Gamma$ and $d$ has been analyzed, and it is found that for the largest value of $\Gamma$, the diffusion coefficient does not increase monotonically with layer separation, but has a distinct minimum for values of $d$ slightly less than 1.

DOI: 10.1103/PhysRevE.65.051203 PACS number(s): 61.20.Ja, 66.10.−x, 64.70.Ja

## I. INTRODUCTION

Two-dimensional electron systems have been extensively studied, both experimentally and theoretically, during the last 20 years. Understanding of such systems has led to important developments in semiconductor technology. Recently, layered structures of charged particles have become a focus of research in theory [1–3], experiment [4], and computer simulation [5,6]. Ion traps and semiconductor devices are examples of such structures; they have been fabricated using nanotechnology techniques for a fairly wide range of densities and interlayer separations. A simple but realistic model of such systems is that of a bilayer, where charged particles are confined to two plane parallel layers, so that each plane contains a one-component plasma (OCP) in a neutralizing uniform background.

Lattice dynamics calculations [1] at zero temperature, (i.e., $\Gamma=\infty$), have shown that a classical bilayer Wigner crystal undergoes a sequence of distinct structural phases as the layer separation is increased from zero. It starts off, as expected, from a monolayer hexagonal lattice and then becomes a staggered rectangular lattice, a staggered square lattice, a staggered rhombic lattice, and finally ends up in the expected staggered hexagonal lattice for values of the interlayer separation greater than 1.3 in units of the Wigner-Seitz (WS) radius.

This bilayer model can be studied using molecular dynamics (MD) simulation methods. Such studies should provide valuable insights into its behavior. Static properties such as intralayer and interlayer pair distribution functions, dynamic properties such as time correlation functions, and transport properties such as diffusion can be obtained from the MD data. In this paper, we deal mainly with self-diffusion of the charged particles, as this plays an important role in understanding the dynamics of such systems and hence in their physical applications. The aim of this paper is to investigate the effect on diffusion of the interlayer separation distance for various values of the coupling strength.

## II. METHOD

The system to be simulated is a bilayer consisting of classical electrons interacting through the three-dimensional Coulomb potential. The electrons are distributed in two planes separated by a constant distance; each electron is constrained to move only in the plane of its original distribution. Charge neutrality is guaranteed by embedding the electrons in a uniform background of opposite charge. A thermodynamic state of the system is entirely specified by the plasma coupling parameter $\Gamma=e^2/ak_BT$ and the interlayer separation $d$; $a=(n\pi)^{-1/2}$ is the WS radius with $n$ being the areal density, $k_B$ is the Boltzmann constant, $e$ is the electronic charge, and $T$ is the temperature. Only symmetric bilayers, in which the density of the electrons is the same in both layers, were considered in this study.

Since the Coulomb potential is of long range, certain modifications have to be made when it is used in a MD simulation. A widely used technique is based on the Ewald sum that has been applied in three-dimensional and two-dimensional OCP studies. This method has been extended to bilayers [7,8], giving the following expression for the force on, say, particle 1 due to particles in the same plane and in the other plane [7].

$$\vec{F}(\vec{r}_1)=\frac{2\pi}{L^2}\sum_{\vec{g}=0}\vec{g}\left\{\frac{1}{g}\,\mathrm{erfc}\left(\frac{g}{2\alpha}\right)\sum_{j=2}^{N}\sin[\vec{g}\cdot(\vec{r}_1-\vec{r}_j)]+\psi(g;\kappa,d)\sum_{j=1}^{N}\sin[\vec{g}\cdot(\vec{r}_1-\vec{\rho}_j)]\right\}+\sum_{\vec{p}}{}'\sum_{j=1}^{N}\frac{\vec{s}_{1j}}{|\vec{s}_{1j}|^3}\left\{\mathrm{erfc}(\alpha|\vec{s}_{1j}|)+\alpha|\vec{s}_{1j}|\,\frac{2}{\sqrt{\pi}}\right.$$

 

$$\times \exp(-\alpha^2|\vec{s}_{1j}|^2)\Bigg\} + \sum_{\vec{p}} \sum_{j=1}^{N} \frac{\vec{d}_{1j}}{|\vec{d}_{1j}|^3}\Bigg\{ \operatorname{erfc}(\kappa|\vec{d}_{1j}|) + \kappa|\vec{d}_{1j}| \frac{2}{\sqrt{\pi}} \exp(-\kappa^2|\vec{d}_{1j}|^2)\Bigg\} \quad (1)$$

with

$$\psi(g;\kappa,d) = \int_0^\infty dr \frac{r}{\sqrt{r^2+d^2}} \operatorname{erf}(\kappa\sqrt{r^2+d^2}) J_0(gr) = \frac{1}{2g}\left[ e^{gd} \operatorname{erfc}\left(\frac{g}{2\kappa}+\kappa d\right) + e^{-gd} \operatorname{erfc}\left(\frac{g}{2\kappa}-\kappa d\right)\right], \quad (2)$$

$\vec{s}_{1j}=\vec{r}_1-\vec{r}_j+\vec{p}$ and $\vec{d}_{1j}=\vec{r}_1-\vec{\rho}_j+\vec{d}+\vec{p}$; $\vec{r}_i$ denotes the position of the $i$th electron in the bottom $(x,y)$ plane and $\vec{\rho}_j$ the position of the $j$th electron in the top $(x,y)$ plane, and the planes are separated by a distance $d$ along the $z$ axis; $L$ is the length of the square simulation cell and $N$ is the number of electrons in each cell. The sum over $\vec{p}$ is a sum over integers $\lambda_1,\lambda_2$ with $\vec{p}=L(\lambda_1,\lambda_2)$; the prime on this sum implies that if $i=j$, the $\vec{p}=\vec{0}$ term is to be omitted. The parameters $\alpha$ and $\kappa$ are to be so chosen that both series in Eq. (1) converge rapidly. Our analysis indicated that a good choice for both of the parameters is $8/L$ and an acceptable accuracy can be obtained using $\sqrt{20}$ for the largest $|\vec{\lambda}|$; this corresponds to taking 38 terms in the $g$-space sums in the expression for the force. This is sufficiently large that only the $\vec{p}=\vec{0}$ terms in the $r$-space summation in Eq. (1) need to be retained, implying that the real-space term vanishes at a distance corresponding to the distance from the cell center to its edge. The dynamics in our MD simulation is based on this expression for the force. All quantities involved are in dimensionless units: distance in units of WS radius $a$, time in units of $\tau=\sqrt{ma^3/e^2}$. The two layers have the same surface density and the basic cell is a square with side length $L=(N/na^2)^{1/2}$, containing 128 electrons in each of the two layers. Since $a$ is the unit of length, the density in each layer takes the value $1/\pi$. For a typical electron density of $8\times10^{12}$ m$^{-2}$, $a$ is $2\times10^{-7}$ m.

The starting configuration for the electrons was a face-centered structure, with velocities given by the Maxwellian distribution determined by the plasma parameter $\Gamma$, (i.e., inverse temperature). The time step $h$ was chosen to be 0.03 in dimensionless units; (this corresponds to about 0.16 ps). Temperature scaling was done every 50 time steps. The starting equilibrium configuration for the MD simulation of interest was obtained after running the initial configuration for 9000 time steps (containing three temperature scaling intervals). We were able to maintain the temperature to within about 2% of the desired temperature in each layer, while conserving the total linear momentum and checking that the total energy was constant during time intervals during which there was no temperature scaling. It is worth stressing that maintaining the temperature in *each* layer is essential, not just in the bilayer system as a whole. (The independence of the total energy on the Ewald sum parameter $\kappa$ was confirmed in [7].)

The position coordinates of the electrons were then computed without temperature scaling for the next 20 000 time steps and stored. The temperature stayed within 2% of the desired value for each separation $d$ considered and each layer. These coordinates were used to obtain the two types of pair distribution function and the mean-square displacement as a function of time. Simulations were performed for $\Gamma=10$, 20, 40, and 80, and various values of $d$ from 0.1 to 3. The pair distribution function $g(r)$ was obtained from the simulation data using the formula

$$\langle n(r)\rangle = 2\pi r \Delta r n g(r), \quad (3)$$

where $\langle n(r)\rangle$ is the average number of particles in an annulus of radius $r$ and thickness $\Delta r$, centred at a given particle. $\Delta r$ was taken to be 0.02, and averages were carried out over 20 000 time steps, with every fifth time step as a new origin. Both the intralayer $g_{11}(r)$, and interlayer $g_{12}(r)$ pair distribution functions were calculated; $g_{11}(r)$ corresponds to particles in the same layer, while $g_{12}(r)$ corresponds to particles belonging to different layers but positions projected onto the same plane.

The diffusion coefficient $D$ can be obtained from the assumed linear behavior of the mean-square displacement at large times. In theory, it can be computed from the relation

$$D = \lim_{t\to\infty} \frac{\langle \Delta r^2(t)\rangle}{4t} = \lim_{t\to\infty} \frac{1}{4}\frac{d}{dt}\langle \Delta r^2(t)\rangle, \quad (4)$$

where

$$\langle \Delta r^2(t)\rangle = \frac{1}{N}\left\langle \sum_{j=1}^{N} |\vec{r}_j(t)-\vec{r}_j(0)|^2 \right\rangle \quad (5)$$

is the mean-square displacement. In practice, we plotted Eq. (5) and $\langle \Delta r^2(t)\rangle/4t$ for each layer and used the latter to estimate the constant $D$. For most states, both layers gave nearly the same plots and we were able to estimate errors in $D$ from these plots.

## III. RESULTS AND DISCUSSION

We have calculated the pair distribution functions $g_{11}(r)$ and $g_{12}(r)$ and the diffusion coefficient for $\Gamma=10$, 20, 40, and 80, for various values of the interlayer separation $d$. However, in this paper we wish to present a detailed analysis of our results for $\Gamma=80$ only. It has been shown, experimentally [9] and by computer simulation [10], that melting of an isolated two-dimensional electron solid occurs in the range $120<\Gamma<140$. Thus, to specifically investigate the sequence of solid-solid structural phase transitions of a classical electronic bilayer as a function of layer separation, a high value of $\Gamma$ is needed. Weis, Levesque, and Jorge [5] have performed Monte Carlo simulations for $\Gamma=196$. At this value of $\Gamma$ the system is in a solid phase, the diffusion coefficient will be extremely small and the mean-square displacement will

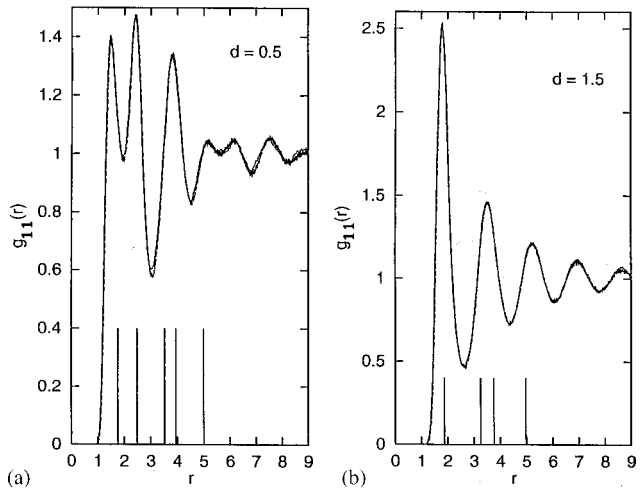


FIG. 1. Intralayer pair correlation function $g_{11}(r)$ for $\Gamma=80$, (a) $d=0.5$ and (b) $d=1.5$. Our results are indicated by solid lines, while those of Donkó and Kalman [6] by dashed lines. The vertical lines indicate the positions of the nearest-neighbor shells for a perfect (a) staggered square lattice and (b) staggered hexagonal lattice. $r$ and $d$ are in units of the Wigner-Seitz radius $a$. Quantities plotted in all figures are dimensionless.

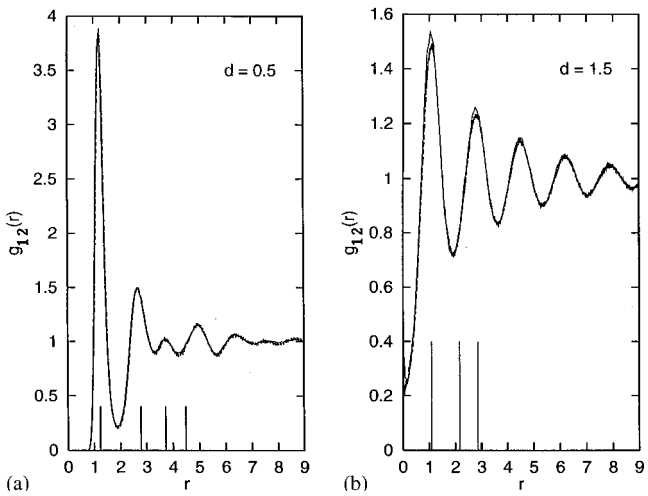


FIG. 2. Same as Fig. 1, except for interlayer pair correlation function $g_{12}(r)$.

show oscillatory behavior. Since our interests lie in an analysis of diffusion, we chose $\Gamma=80$. For this value, the bilayer system would be in a fluid phase of an equivalent, isolated two-dimensional OCP for small and large values of interlayer separation, but still the effects of solidlike behavior in diffusion could be seen at certain intermediate values of the interlayer separation.

In Figs. 1(a) and 1(b) the results for intralayer pair correlation function $g_{11}(r)$ for $\Gamma=80$ and for $d=0.5$ and 1.5 are shown. The solid line represents our results and the dashed line the results of Donkó and Kalman [6]. They calculated $g_{11}(r)$ and $g_{12}(r)$ for an electronic bilayer using an MD simulation based on the (particle-particle particle-mesh) algorithm while we have used an algorithm that is an extension of the Ewald sum for a two-dimensional OCP. It is seen that the two MD results agree very well and establish the fact that both algorithms are correct and accurate. We have compared the two results for a range of $\Gamma$ and $d$ values and the agreement is excellent throughout.

The vertical lines in Fig. 1(a) denote the peak positions of the nearest-neighbor shells of a perfect square lattice, while in Fig. 1(b) they denote the peak positions of the nearest-neighbor shells of a perfect hexagonal lattice. These positions have been taken from the results of Weis Levesque, and Jorge [5]. Thus we see changes in lattice structures, even though the system is not quite in a solid phase. At $d=0.5$, the peak positions of $g_{11}(r)$ do reflect those of a square lattice. At $d=1.5$, the peak positions have clearly moved away from that of a square lattice and are now more suggestive of a hexagonal lattice. The agreement between the peak positions of $g_{11}(r)$ and those of the lattices will not be precise, as the value of $\Gamma$ is only 80 and thus considerably less than the solid changeover value.

In Figs. 2(a) and 2(b), similar results for the interlayer pair correlation function $g_{12}(r)$ are shown. It should be recalled that $g_{12}(r)$ relates to particles belonging to different layers but with their positions projected onto one plane. Again the agreement between the two MD results is excellent. The vertical lines indicate the peak positions of a perfect staggered square lattice at $d=0.5$, and that of a perfect staggered hexagonal lattice at $d=1.5$. Note that these positions are different from those in Fig. 1.

Though the system at $\Gamma=80$ is quite removed from the transition to a solid for small and large interlayer separations, both pair correlation functions do display a variety of interesting features as the interlayer separation changes. These correlation functions have been generated earlier using the hypernetted chain theory [2] and by molecular dynamics [6], and have been discussed and analyzed [2,6], but still it is worthwhile, for the sake of completeness, to just point out some of their salient features.

(a) At $d=0.1$, $g_{11}(r)$ and $g_{12}(r)$ are very nearly the same, and they agree with the $g(r)$ expected from a single isolated layer with $\Gamma=80\sqrt{2}\cong 113$. At $d=0$, the two layers merge, thus doubling the density and hence the system behaves like an isolated two-dimensional layer, with $\sqrt{2}\Gamma$ as its plasma parameter. The peak positions reveal the expected hexagonal structure, though not exactly, since $\Gamma$ is still lower than the solidification value of about 130.

(b) As $d$ is increased to about 0.5, the height of the first peak of $g_{11}(r)$ decreases considerably and actually becomes less than the height of the second peak. In the same interval, the height of the first peak of $g_{12}(r)$ increases considerably. The structure has slowly changed from hexagonal to square.

(c) As $d$ increases from 0.5 to about 1.0, the heights and positions of the peaks in $g_{11}(r)$ and $g_{12}(r)$ rearrange, as the system is trying to evolve into a hexagonal lattice. As $d$ further increases, there are no significant changes in $g_{11}(r)$ as it keeps the hexagonal structure, loses some of its long-range characteristics and gets closer to the $g(r)$ of an isolated layer with $\Gamma=80$. For $d>2$, there is no appreciable correlation between the two layers and $g_{12}(r)$ loses all of its structure.

These structural changes are also reflected in the heights

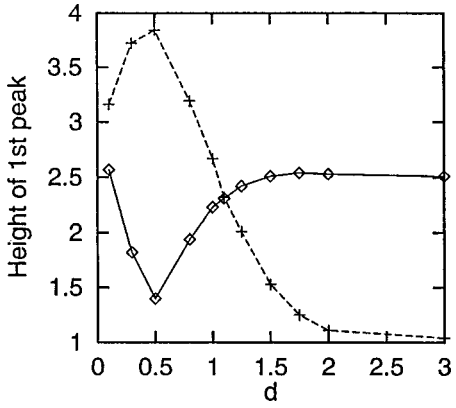


FIG. 3. Dependence on the interlayer separation $d$, of height of first peak for $g_{11}(r)$ (solid) and $g_{12}(r)$ (dashed) for $\Gamma=80$.

of the first peaks of the pair correlation functions. Figure 3 is a plot showing the height of the first peak of $g_{11}(r)$ and $g_{12}(r)$ as a function of the interlayer separation $d$ for $\Gamma=80$. It is seen that one graph is almost a mirror image of the other for $d<1$. The height of the first peak of $g_{11}(r)$ goes through a minimum while that for $g_{12}(r)$ attains a maximum. The maximum height of the first peak for $g_{12}(r)$ occurs near $d=0.5$. Since the height is an indication of the coordination numbers, the plot is suggestive of structural changes.

Figures 4(a) and 4(b) are plots showing the mean-square displacement as a function of time for $\Gamma=80$. The first shows approximately straight lines with slopes that decrease as $d$ increases for some values of $d$ in [0.1, 0.65]. The second indicates that for $d$ in [0.65, 0.9] the diffusion rate is much smaller and the mean-square displacement shows oscillations with time. Such behavior is typical of the small diffusion rates and the structure found in solids. The values of $d$ for which this occurs are in the domain where the bilayer is in a staggered square structure.

Figure 5 illustrates the variation of the diffusion coefficient $D$ with interlayer separation $d$ for $\Gamma=80$. We have noted that for $d=0$, and for $d>2$, the system behaves like an isolated two-dimensional layer. However for $d=0$, the value of the plasma parameter $\Gamma$ is 113, while for $d>2$, $\Gamma$ is 80. Since diffusion coefficients increase as $\Gamma$ decreases, one might expect a monotonic increase in the diffusion coefficient as the interlayer separation increases. However, our results show a very different and dramatic behavior. The diffusion coefficient starts at $d=0.1$ with a value that closely corresponds an isolated layer with $\Gamma=113$. It then decreases, *by an order of magnitude*, as the interlayer separation $d$ increases to 0.8, after which it shows a very quick increase and then levels off, for $d>1.5$, at a value that corresponds to an isolated layer with $\Gamma=80$. Such a behavior reflects the fact that our chosen value of $\Gamma$ is high enough to initiate crystalline phases for certain interlayer separations. The drastic reduction of the diffusion coefficient in the range $0.5<d<1.0$ clearly indicates the enhanced stability of the staggered square lattice structure in this domain. It can be argued that this is indicative of a solid-liquid phase transition in the $\Gamma$-$d$ plane, but more research along these lines has to be done for

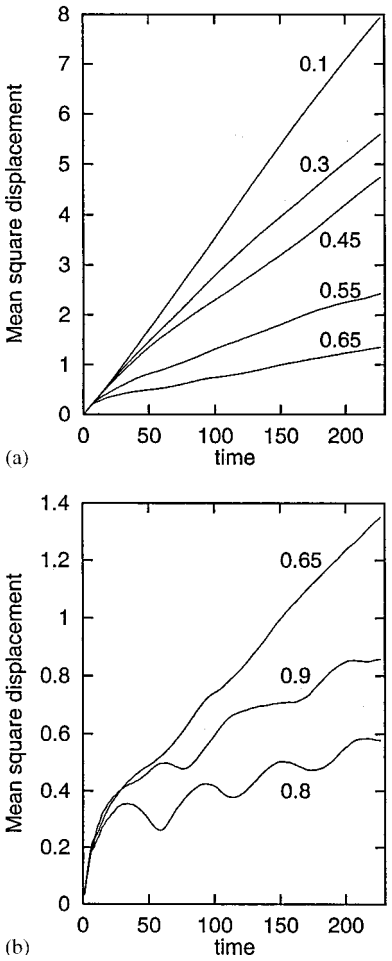


FIG. 4. Mean-square displacement (in units of $a^2$) as function of time (in units of $\tau$) for $\Gamma=80$. (a) $d$ values between 0.1 and 0.65. (b) $d=0.65$, 0.8, and 0.9.

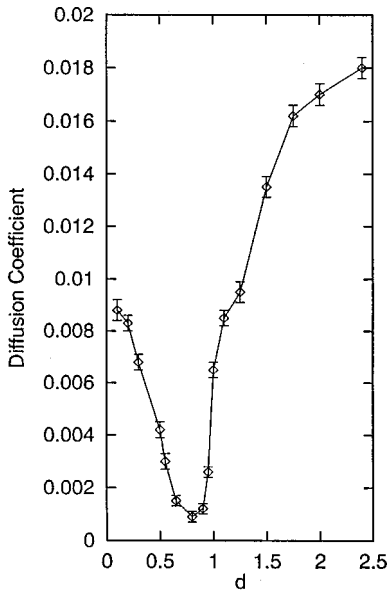


FIG. 5. Dependence of diffusion coefficient $D$ (in units of $a^2/\tau$) on layer separation $d$ (in units of $a$) for $\Gamma=80$.

various values of $\Gamma$ to map out the phase boundary completely.

We have also indicated error bars in Fig. 5 in the calculation of $D$, for each value of the interlayer separation. The main sources of error are the variation in the temperature of each layer during the simulation resulting in a slightly different diffusion behavior of the layers and the fact that simulations produce mean-square displacements that are not, for long times, exactly linear functions of time for some values of $d$. Nevertheless, the nature of the dependence of the diffusion coefficient on interlayer separation is unequivocally revealed in this diagram.

In conclusion, we note that for small and large values of $d$, the pair distribution functions mirror that of a fluid phase; at intermediate values of $d$, the two layers support each other to establish a long-range order and create crystalline phases. The formation of crystalline structures would indeed decrease the diffusion coefficient. It is seen that though the system undergoes hexagonal, rectangular, square, rhombic, and back to hexagonal structures as the layer separation increases, the diffusion coefficient shows a decrease only up to the formation of a square lattice for our chosen value of $\Gamma$. Note that crystalline phases for an isolated two-dimensional OCP, would not be detected until $\Gamma$ is larger than 130. The behavior of the diffusion coefficient as a function of the layer separation is the main result of our paper and it would be interesting to extend this research to a wide range of $\Gamma$ values. One can then analyze the stability of the various lattice structures, their effect on diffusion, and the existence of a solid-liquid phase boundary in the $\Gamma$-$d$ plane. Our results should also provide impetus to devise experiments that would measure diffusion coefficients and to develop theoretical models of diffusion in classically charged bilayers.

## ACKNOWLEDGMENTS

This project was supported in part by a grant from the Academic Research Program (ARP) of the Department of National Defence, Canada. We thank Z. Donkó and G. Kalman for providing their $g(r)$ data.

[1] G. Goldoni and F. M. Peeters, Phys. Rev. B **53**, 4591 (1995).
[2] V. I. Valtchinov, G. Kalman, and K. B. Blagoev, Phys. Rev. E **56**, 4351 (1997).
[3] K. I. Golden, G. Kalman, and Ph. Wyns, Phys. Rev. A **41**, 6940 (1990).
[4] J. J. Bollinger, T. B. Mitchell, X.-P. Huang, W. M. Itano, J. N. Tan, B. M. Jelenković, and D. J. Wineland, Phys. Plasmas **7**, 7 (2000).
[5] J.-J. Weis, D. Levesque, and S. Jorge, Phys. Rev. B **63**, 045 308 (2001).
[6] Z. Donkó and G. Kalman, Phys. Rev. E **63**, 061504 (2001).
[7] R. E. Johnson and S. Ranganathan, Phys. Rev. E **63**, 056 703 (2001).
[8] B. Cichocki and B. U. Felderhof, Mol. Phys. **67**, 1373 (1989).
[9] C. G. Grimes and G. Adams, Phys. Rev. Lett. **42**, 795 (1979).
[10] R. K. Kalia, P. Vashishta, and S. W. de Leeuw, Phys. Rev. B **23**, 4794 (1981).